Materials Research Proceedings **26** (2023) 17-22 https://doi.org/10.21741/9781644902431-3

A variational model for plastic reorientation in fibrous material: numerical experiments on phase segregation

Andrea Rodella[1, a *], Antonino Favata[1,b] and Stefano Vidoli[3,c]

[1]DISG, "Sapienza" University of Rome, Via Eudossiana 18, 00185 Rome, Italy

[a]andrea.rodella@unitoma1.it, [b]antonino.favata@uniroma1.it, [c]stefano.vidoli@uniroma1.it

Keywords: Phase Segregation, Fibrous Material, Plastic Remodeling, FEniCS

Abstract. We propose a continuum model of fibrous material that may undergo an internal reorganization, which turns out in a plastic change of the orientation of the fibers when the remodeling torque achieves a threshold. We have recently found that the reorientation may induce a complex scenario in the response of such materials. In a traction test, we show that the most general transversely isotropic material may evolve in three different ways; in particular, the fibers asymptotically tend (regularly or with jumps): (*A*) to a given angle; (*B*) to align perpendicularly to the load direction; (*C*) to align with the load direction if their initial orientation is less than a given value otherwise perpendicularly. We focus on the latter material response (*C*) which has all the ingredients to manifest a phase transition phenomenon. Finally, we provide a numerical investigation to demonstrate phase segregation.

Introduction

Due to their ubiquity, fibrous materials have gained a predominant role in the scientific community in the last few decades. Fibrous structures are everywhere; the human body is a glaring example: the connective tissue, the most abundant tissue in mammals, is composed mainly of extracellular matrix and collagen fibers (∼6% of the total body weight). It is also well established that biological tissues may experience an internal reorganization, including segregation [1], due to external stimuli at chemo-mechanical levels. This phenomenon corresponds to a change in the fiber orientation that may be associated with a loss of the elastic energy content, resulting in irreversible deformations [2]. The effects of reorientation, particularly those occurring during the post-yield deformation, remain largely unexplored in biological and manufactured composites despite their fundamental role in the mechanical response [3]. We focus on the most general 2D transversely isotropic material to model the plastic reorientation in fibrous materials. Then, we consider a linearized framework concerning the strain measure; nevertheless, we admit finite rotation for the fibers. Within a thermodynamically consistent framework [4], we present a variational model taking into account the anisotropic response of the material, which depends on an internal variable, *e.g.*, the fiber orientation. The latter, similarly to plasticity [5], has the peculiarity to evolve till a threshold beyond which the reorientation is permanent. We recall the main analytical results of the incremental homogenous traction problem we recently found in [6]. In this work, we show three different asymptotic behavior for the orientation of the fibers, which tend to align, smoothly or not: *(A)* with a given angle; *(B)* perpendicularly with the load direction and *(C)* perpendicularly with the load direction or with the load direction itself in accordance with the initial orientation. The energy of the material in class *(C)* presents a double-well landscape which may induce a phase transition and give room for exploring the phase segregation.

We organize the work as follows: i) we present the assumptions to formulate a thermodynamically consistent phase-field model taking into account the anelastic response of the material; ii) we recall the main analytical results found in [6] for the traction test; iii) we provide some numerical results for a non-homogeneous initial fiber orientation distribution showing the evolution of the traction test leading to the segregation phenomenon.

Materials Research Proceedings **26** (2023) 17-22 https://doi.org/10.21741/9781644902431-3

Assumptions for the free energy and the reversibility domain

For the sake of simplicity, we confine our analysis to a two-dimensional body $\mathcal{B}$. The vector position of the point $x \in \mathcal{B}$ is defined as $\mathbf{x} = x - o = x_a\,\mathbf{e}_a$ with respect to the origin o of the Cartesian frame $\{o,\ \mathbf{e}_1,\ \mathbf{e}_2\}$. We chose to associate an orientated fiber to each material point in $\mathcal{B}$, whose direction is represented by the unit vector $\mathbf{n}(\vartheta) = \cos\vartheta\,\mathbf{e}_1 + \sin\vartheta\,\mathbf{e}_2$ as a function of the *internal state variable* ϑ . Recalling [4,7,8], the state variable influences the free energy and the dissipation rests upon the evolution of ϑ. The state for the body $\mathcal{B}$ at each time t is known if the list of functions of the spatial coordinate x, $\mathbf{\Lambda} = \{\mathbf{E}, \vartheta\}$ is known, where $\mathbf{E} = \mathrm{sym}\nabla\mathbf{u}$ is the linearized strain measure expressed in terms of the displacement field $\mathbf{u}$. The free energy density is taken as a quadratic form of the strain field

$$\psi = \hat{\psi}(\mathbf{E}, \vartheta) = \frac{1}{2}\mathbb{C}\big(\mathbf{n}(\vartheta)\big)\mathbf{E}\cdot\mathbf{E}, \tag{1}$$

where $\mathbb{C}\big(\mathbf{n}(\vartheta)\big)$ represents the elasticity tensor of a linearly elastic transversely isotropic material with respect to the direction $\mathbf{n}(\vartheta)$. For the most general two-dimensional case, we specify the free energy density as follows:

$$\hat{\psi}(\mathbf{E}, \vartheta) = \mu\|\mathbf{E}\|^2 + \frac{\lambda}{2}(\mathrm{tr}\mathbf{E})^2 + c_1(\mathrm{tr}\mathbf{E})\mathbf{E}\mathbf{n}(\vartheta)\cdot\mathbf{n}(\vartheta) + c_2\big(\mathbf{E}\mathbf{n}(\vartheta)\cdot\mathbf{n}(\vartheta)\big)^2, \tag{2}$$

where λ and μ are the Lamé coefficients and c_1 and c_2 are the material constants characterizing the transversely isotropy. By fixing the Lamé coefficients, which must respect the conditions $\mu > 0$ and $2\mu + \lambda > 0$, the pair of constants (c_1, c_2) must lie in a set $\mathcal{P}$, ensuring the positiveness of the energy Eq. (2)

$$\mathcal{P} = \left\{c_1, c_2 \in \mathbb{R}\colon c_2 > \frac{c_1^2 - 4\mu c_1 - 4\mu(\mu+\lambda)}{2(2\mu+\lambda)}\right\}, \tag{3}$$

which represents a parabola, see Fig. 1. In order to clarify the role of the constant c_1 and c_2 on the anisotropic material response, it is useful to recall the definitions of Young modulus and Poisson ratio, defined for a uniaxial traction test $\overline{\mathbf{T}} = \sigma\mathbf{t}\otimes\mathbf{t}$ in the direction $\mathbf{t} = \cos\alpha\,\mathbf{e}_1 + \sin\alpha\,\mathbf{e}_2$. The strain corresponding to $\overline{\mathbf{T}}$ is defined as $\overline{\mathbf{E}} = \mathbb{C}^{-1}\big(\mathbf{n}(\vartheta)\big)\overline{\mathbf{T}}$. Therefore, the Young modulus and the Poisson ratio are functions of the angle resulting from the difference between the testing direction and the fiber orientation $(\alpha - \vartheta)$ and follow the definitions:

$$E(\alpha, \vartheta) = \hat{E}(\alpha, \vartheta) \coloneqq \frac{\overline{\mathbf{T}}\mathbf{t}\cdot\mathbf{t}}{\overline{\mathbf{E}}\mathbf{t}\cdot\mathbf{t}}; \qquad \nu(\alpha, \vartheta) = \hat{\nu}(\alpha, \vartheta) \coloneqq \frac{\overline{\mathbf{E}}\mathbf{t}^{\perp}\cdot\mathbf{t}^{\perp}}{\overline{\mathbf{E}}\mathbf{t}\cdot\mathbf{t}}. \tag{4}$$

Polar plots are, therefore, a meaningful tool to understand how Young modulus and Poisson ratio change in function of the angle $(\alpha - \vartheta)$, see the insert in Fig. 1. We define the stiffening set $\mathcal{S}$ by imposing the ratio between the Young modulus in the parallel and perpendicular with respect to the fiber direction $E_{||} = \hat{E}(\alpha = \vartheta, \vartheta)$ and $E_{\perp} = \hat{E}(\alpha = \vartheta - \pi/2, \vartheta)$ to be greater than 1:

$$E_{\parallel}/E_{\perp} = 1 + \frac{2(c_1+c_2)}{2\mu+\lambda} > 1 \quad \Longrightarrow \quad \mathcal{S} = \{c_1, c_2 \in \mathcal{P}\colon c_1 + c_2 > 0\} \tag{5}$$

Materials Research Proceedings **26** (2023) 17-22 https://doi.org/10.21741/9781644902431-3

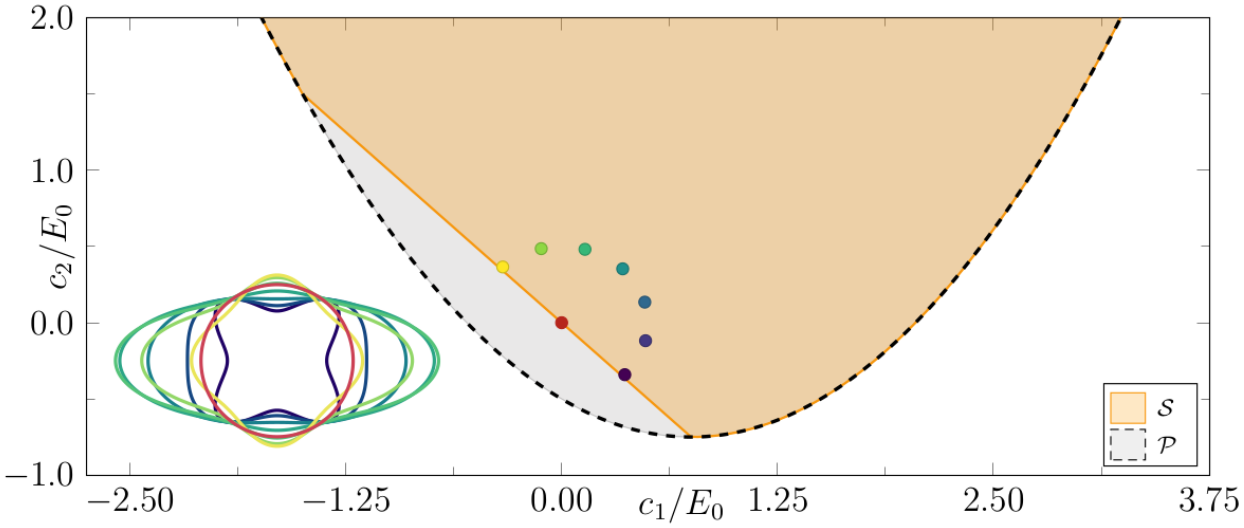

***Figure 1**: The gray area confined by the black dashed line represents the set where the pair $\{c_1, c_2\}/E_0$ ensures the positiveness of the energy, see Eq. (3), where E_0 is the Young modulus of the isotropic case. While the yellow area represents the stiffening set, a subset of $\mathcal{P}$, obeying Eq. (5). The insert figure is the polar plot of the Young modulus $\hat{E}(\alpha, \vartheta = 0)$ where $\alpha \in [0,2\pi]$. Each polar plot corresponds to the colored dot picked from the stiffening set $\mathcal{S}$.*

In the framework of *Generalized Standard Materials* [4], the dissipative behavior is described through the dissipation potential, which is a convex and positive function of the internal state variables rates. Since $\mathbf{n} \cdot \mathbf{n} = 1$, we have $\dot{\mathbf{n}} \cdot \mathbf{n} = 0$ or, equivalently, $\dot{\mathbf{n}} = \beta \mathbf{n}^{\perp}$ with $\mathbf{n}^{\perp} := \partial_{\vartheta}\mathbf{n}(\vartheta) = -\sin\vartheta\, \mathbf{e}_1 + \cos\vartheta\, \mathbf{e}_2$, from Eq. (2), the energy release rate turns out to be

$$\begin{aligned} -\partial_{\vartheta}\hat{\psi}(\mathbf{E}, \vartheta)\dot{\vartheta} &= -\partial_{\mathbf{n}}\hat{\psi}\big(\mathbf{E}, \mathbf{n}(\vartheta)\big) \cdot \dot{\mathbf{n}}(\vartheta) \\ &= -2\big(c_1 \mathrm{tr}\mathbf{E} + 2c_2 \mathbf{E}\mathbf{n}(\vartheta) \cdot \mathbf{n}(\vartheta)\big)\mathbf{E}\mathbf{n}(\vartheta) \cdot \beta \mathbf{n}^{\perp}(\vartheta) \\ &= -\beta\gamma(\mathbf{E}, \vartheta) \end{aligned} \tag{6}$$

where $\gamma(\mathbf{E}, \vartheta)$ is the force thermodynamically associated to the change of fiber orientation ϑ, hereafter named *remodeling torque*. In order to respect the fundamental inequality [4], the energy release rate in Eq. (6) calculated at $\mathbf{E}$ must be greater than the energy release rate calculated at any other admissible $\tilde{\mathbf{E}}$:

$$-\beta\big[\gamma(\mathbf{E}, \vartheta) - \gamma\big(\tilde{\mathbf{E}}, \vartheta\big)\big] > 0 \tag{7}$$

for any $\mathbf{E}$ and $\tilde{\mathbf{E}}$ in the reversibility domain, $\mathcal{R}(\eta)$. This latter is the set of the symmetric strain tensors that make the remodeling torque stay below the critical material threshold $\eta > 0$:

$$\mathcal{R}(\eta) = \left\{ \mathbf{E} \in \mathbb{S}\mathrm{ym}: \sup_{\vartheta \in [-\pi/2,\ \pi/2]} |\gamma(\mathbf{E}, \vartheta)| \leq \eta \right\}. \tag{8}$$

Equivalently, this set can also be interpreted as the strains for which the fiber orientation ϑ cannot evolve, and the material response is purely elastic. Finally, by following [4,5], the dissipation rate is given through the Legendre transform:

$$d(\vartheta)\big(\dot{\vartheta}\big) = \sup_{\mathbf{E} \in \mathcal{R}(\eta)} \big(-\partial_{\vartheta}\hat{\psi}(\mathbf{E}, \vartheta)\dot{\vartheta}\big) = \eta\beta\big|\dot{\vartheta}\big| = \bar{\eta}\big|\dot{\vartheta}\big|. \tag{9}$$

Materials Research Proceedings **26** (2023) 17-22 https://doi.org/10.21741/9781644902431-3

Now, by considering a quasi-static process over a time interval observation t, the total dissipation is defined as

$$\delta = \hat{\delta}(t) = \int_0^t d(\vartheta(\tau))\big(\dot{\vartheta}(\tau)\big)d\tau = \bar{\eta}\int_0^t \big|\dot{\vartheta}(\tau)\big|d\tau =: \bar{\eta}\overline{\Theta}(\mathrm{t}), \tag{10}$$

where the dependency with respect to the time t has been highlighted; $\overline{\Theta}(t)$ represents the accumulated fiber rotation over the time interval t. The total energy is, then, defined by integrating the free energy density Eq. (1) plus the remodeling dissipation Eq. (10) over the body

$$\mathcal{E}(\mathbf{E}(t),\vartheta(t)) = \int_{\Omega}\big(\hat{\psi}(\mathbf{E}(t),\vartheta(t)) + \hat{\delta}(t)\big)dA. \tag{11}$$

Traction problem

We examine the traction problem sketched in Fig. 2(a). A rectangular sample, of length L and height H, is left free on the upper and lower sides and free to slide on the left side; the horizontal displacement of the points on the right side is equal to $\bar{\mathbf{u}} = \varepsilon L\mathbf{e}_1$, whilst their vertical displacement is left free.

The present section consists of two parts: the first is dedicated to briefly recalling the analytical results obtained in our recent work [6], while the second focuses on the main objective of this paper: the numerical observation of the segregation phenomenon.

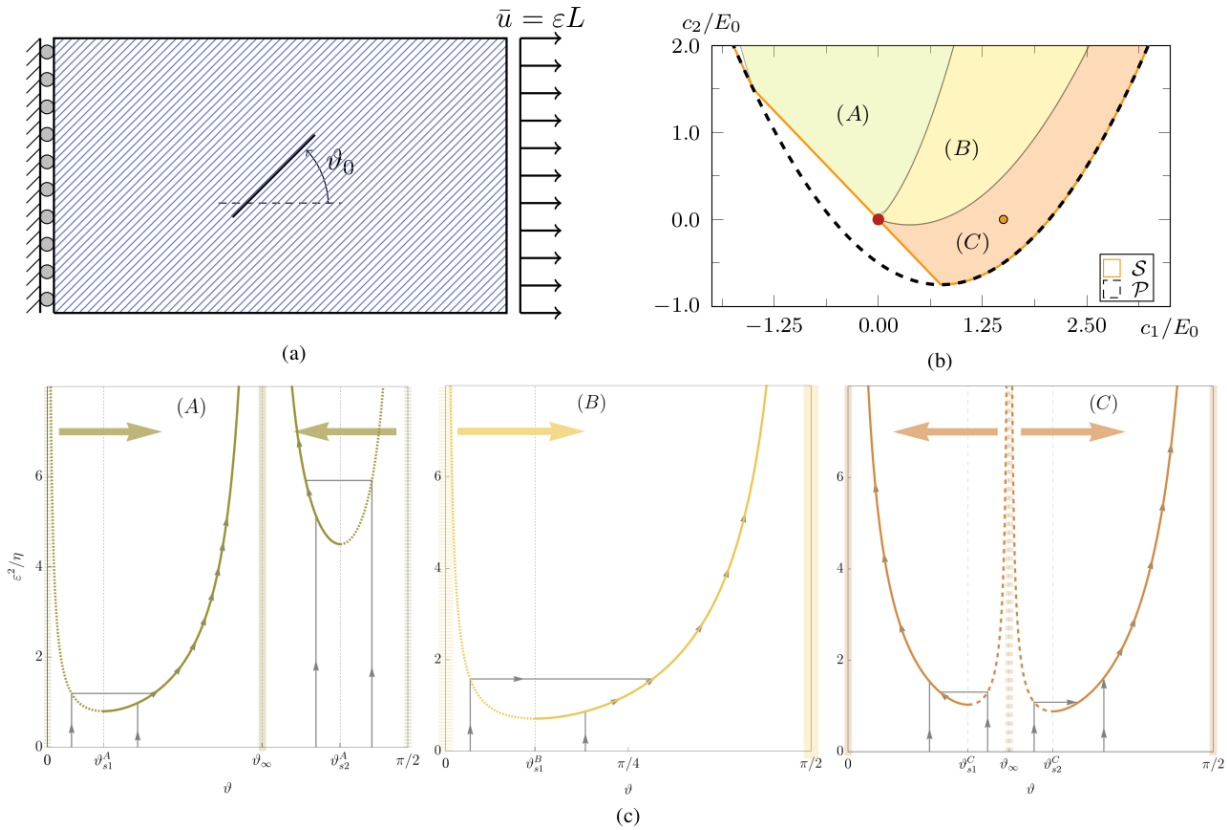

Figure 2: *(a) Schematics of the traction test, ϑ_0 represents the initial fiber orientation, $\bar{u}$ is the imposed displacement acting on the left side of the sample. (b) In the stiffening set $\mathcal{S}$ three different materials are highlighted. (c) ϑ evolution paths (gray continuos lines with arrows) for each case for the three different domains of (b): (A) left, (B) center, and (C) right. Dashed lines represent unstable branches that make the initial fiber orientation jump to the stable branches when the elastic limit is reached.*

Materials Research Proceedings **26** (2023) 17-22 https://doi.org/10.21741/9781644902431-3

Analytical solution for the homogeneous case In [6] it is presented a complete analytical characterization of the homogeneous case in terms of strain and fiber rotation, as the imposed horizontal displacement $\bar{u} = \varepsilon L$ monotonically increases starting from 0. Hence, it is possible to find an asymptotic value of the fiber orientation $\vartheta_\infty(\lambda, \mu, c_1, c_2)$ for $\varepsilon \to \infty$. The stiffening materials are identified in three classes, see Fig. 2(b):

- class (A) presents a minimum of the elastic energy ψ in correspondence of $0 \leq \vartheta_\infty \leq \pi/2$[1] and two maxima $\vartheta = \{0, \pi/2\}$. The evolution of the homogeneous traction problem with an initial uniform fiber orientation $\vartheta_0 \in [0, \pi/2]$ is depicted in Fig. 2(c) left. The fiber orientation evolves with jumps if ϑ_0 has been taken on an unstable branch ($0 \leq \vartheta_0 < \vartheta_{s1}^A$ or $\vartheta_{s2}^A \leq \vartheta_0 < \pi/2$), or continuously if ϑ_0 is initially on a stable branch ($\vartheta_{s1}^A \leq \vartheta_0 < \vartheta_\infty$ or $\vartheta_\infty < \vartheta_0 \leq \vartheta_{s2}^A$).
- class (B) presents the only minimum of ψ at $\vartheta = \pi/2$; $\vartheta = 0$ is, instead, the maximum. Moreover, ϑ_∞ does not exist in $\mathbb{R}$, see Fig. 2(c) center.
- class (C) presents two minima of ψ at $\vartheta = \{0, \pi/2\}$, while ϑ_∞ exists and corresponds to the maximum, see Fig. 2(c) right. In this scenario, it is then possible to observe the segregation in two phases of the fiber orientation, which is the objective of the numerical simulations presented in the next section.

Phase segregation The Lamé constants are chosen $\lambda = \mu = 3/8$ in order to have a unitary Young modulus $E_0 = 1$ and Poisson ratio $\nu_0 = 1/3$. The anisotropic parameters $c_1 = 1.5$ and $c_2 = 0$ are chosen in region (C); see the orange dot in Fig. 2(b). We present three study cases where we consider the evolutions of different non-uniform distributions of initial orientation.

- In Fig.s 3(a-d) are displayed the results obtained by tacking into account an initial linear distribution of orientation $\vartheta_0(\mathbf{x})$ that goes from 9° on the left side to 22° on the right one, Fig. 3(a). This specific non-homogeneous distribution is collocated below the ϑ_∞. The imposed displacement grows until the incipient touching of the yield surface Fig. 3(b). The orientation of the fiber starts to decrease with or without jumps; Fig. 3(c) shows one of those intermediate steps. Eventually, the fibers reach a uniform distribution decreasing toward 8°, Fig. 3(d). At this point, the analytical solution, see Fig. 2(c) left, describes the evolution of the orientation until 0°, that is the closest minimum of the elastic energy.
- Fig.s 3(e-h) describe a sample with a distribution of fiber orientated from 52° to 72°. The evolution is similar to the previous one, but in this case the initial distribution $\vartheta_0(\mathbf{x}) > \vartheta_\infty$. Therefore, the fibers tend to reach the minimum collocated at 90° once the elastic limit is overcome, Fig. 3(g). Again, once the field ϑ reaches homogeneity, see Fig. 3(h), the analytical solution provides the evolution.
- Finally, Fig.s 3 from (i) to (l) show the orientation evolution for a sample in which the initial distribution is $\vartheta_0(\mathbf{x}) = (\pi/2)(x_1/L)$. In this case, ϑ_∞ is a value comprised in the initial distribution, expecting the rotation of the fibers going toward the two minima at 0° and 90°. Snapshot (k) shows the beginning of this process, while snapshot (i) shows the left part of the sample completely segregate with respect to the right one. The left part has the fibers initially orientated above $\vartheta_\infty = 30°$.

Conclusions

We have presented a variational model describing the reorientation in a transversely isotropic material. Similarly to plasticity, the model considers the irreversibility of an internal variable, *e.g.*, the fiber orientation, when the remodeling torque reaches a threshold. Then, we focused on the traction problem by recalling the essential analytical findings for the homogeneous case.

[1] It suffices to consider $\vartheta \in [0, \pi/2]$ as $\vartheta \equiv \vartheta + \pi$ and, for the symmetry of the problem, $\vartheta \equiv -\vartheta$.

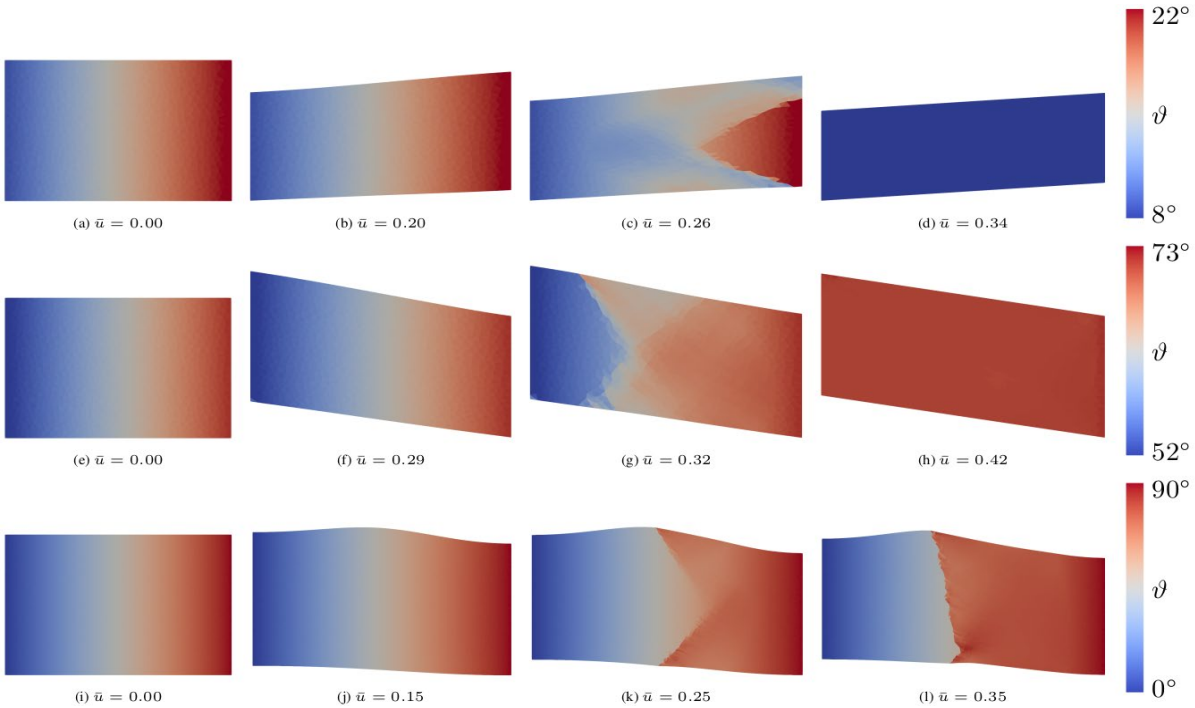

Figure 3: Sequences for a stiffening non-homogeneous material in class (C) characterized by $\boldsymbol{\vartheta_\infty = 30°}$ *with different initial linear distribution of* $\boldsymbol{\vartheta}$*. Sequence from (a) to (d) has* $\boldsymbol{\vartheta_0(x) < \vartheta_\infty \forall x \in \mathcal{B}}$ *. Sequence from (e) to (h) has* $\boldsymbol{\vartheta_0(x) > \vartheta_\infty \forall x \in \mathcal{B}}$*. Finally (i)-(l) has* $\boldsymbol{\vartheta_0(x) = (\pi/2)(x_1/L)}$*.*

It has been possible to divide the material responses into three categories based on their energetic characteristics. Materials in class (*C*), characterized by double-well energy, are suitable for observing phase transitions and, eventually, segregation. In this context, we have presented a numerical case study where an initial inhomogeneous distribution of fiber orientation leads to the segregation of the internal variable.

References

[1] G. Grekas, M. Proestaki, P. Rosakis, J. Notbohm, C. Makridakis, and G. Ravichandran, Cells exploit a phase transition to mechanically remodel the fibrous extracellular matrix, Journal of the Royal Society Interface, vol. 18, no. 175, p. 20200823, (2021). https://doi.org/10.1098/rsif.2020.0823

[2] E. Ban, J. M. Franklin, S. Nam, L. R. Smith, H. Wang, R. G. Wells, O. Chaudhuri, J. T. Liphardt, and V. B. Shenoy, Mechanisms of Plastic Deformation in Collagen Networks Induced by Cellular Forces, Biophysical Journal, vol. 114, no. 2, pp. 450–461, (2018). https://doi.org/10.1016/j.bpj.2017.11.3739

[3] B. Buchmann, L. Engelbrecht, P. Fernandez, et al., Mechanical plasticity of collagen directs branch elongation in human mammary gland organoids, Nature Communication, vol. 12, no. 2759, (2021). https://doi.org/10.1038/s41467-021-22988-2

[4] B. Halphen and Q. Nguyen, Sur les matériaux standards généralisés, Journal de Mécanique, vol. 14, pp. 39–63, 01 (1975).

[5] J.-J. Marigo, Constitutive relations in plasticity, damage and fracture mechanics based on a work property, Nuclear Engineering and Design, vol. 114, pp. 249–272, (1989). https://doi.org/10.1016/0029-5493(89)90105-2

[6] A. Favata, A. Rodella, and S. Vidoli, An internal variable model for plastic remodeling in fibrous materials, European Journal of Mechanics - A/Solids, p. 104718, (2022). https://doi.org/10.1016/j.euromechsol.2022.104718

[7] B. Coleman and M. Gurtin, Thermodynamics with internal state variables, The Journal of Chemical Physics, vol. 47, no. 2, pp. 597–613, (1967). https://doi.org/10.1063/1.1711937

[8] P. Germain, The method of virtual power in continuum mechanics. Part 2: Microstructure, SIAM Journal on Applied Mathematics, vol. 25, no. 3, pp. 556–575, (1973). https://doi.org/10.1137/0125053